CONF-781121--3



# THE DEVELOPMENT OF PROCESS AND STORAGE MATERIALS SUITABLE FOR KRYPTON-85 WASTE MANAGEMENT

T. R. Pinchback, EG&G Idaho, Inc.
and
D. A. Knecht, Allied Chemical Corp.

Idaho Falls, Idaho 83401

## INTRODUCTION

Federal regulations require that no more than 14% of the krypton-85 produced in nuclear fuel after 1983 be released to the atmosphere (1). If these regulations are applied to existing defense nuclear fuel reprocessing plants or if commercial fuel should be reprocessed, techniques for the removal and storage of krypton-85 must be developed.

Krypton-85 may be stored as a pressurized gas or as a solid after immobilization in zeolite. Containment for either the gaseous or the solid forms must be provided for 50-100 years. The process equipment used for recovery and immobilization would be exposed to krypton-85 continually for a 30-40 year period.

The krypton-85 decay product, rubidium, and other gas impurities such as oxygen, $NO_x$ and water, are potential sources of corrosive degradation to materials used in krypton-85 storage containers, valves, and process equipment. Impurities may react with liquid rubidium generated by beta decay of krypton-85 to produce oxide or hydroxide compounds.

A test program is in progress to evaluate the compatibility of candidate construction materials with liquid rubidium and rubidium compounds. Several preliminary screening tests have been completed. Objectives of these screening tests were:

1) Identification of corrosion problems for materials exposed to liquid rubidium in the temperature range proposed for krypton-85 gas cylinder storage (400-672 K).

## DISCLAIMER

2) Identification of liquid metal embrittlement effects for materials exposed to liquid rubidium in the temperature range proposed for krypton-85 gas cylinder storage.

3) Determination of the corrosion kinetics for 304 stainless steel exposed to liquid rubidium in the temperature range proposed for krypton-85 encapsulation in zeolite (793-893 K).

## TEST PROCEDURES

Stressed "C" rings (2) were selected for initial screening exposures in liquid rubidium, since this test provides a simple, low-cost method of determining corrosion and embrittlement problems (objectives 1 and 2) for the candidate materials. The materials tested included:

| | |
|---|---|
| 4130 steel | Nitronic 50 |
| 304 stainless steel | A286 |
| 316 stainless steel | Monel 400 |
| 347 stainless steel | Inconel 600 |

### "C" Ring Tests

Specimens of each material were totally immersed in liquid rubidium (99.9% purity) which partially filled a sealed 1-litre cylinder. The atmosphere over the liquid rubidium was argon with a dew point of 210 K and 1-2 ppm total oxygen. Four such cylinders were fabricated and heated at 400, 491, 573, and 672 K for times between 4,000 and 5,000 hours. Following corrosion exposure, samples were evaluated using the following methods:

1) Visual examination

2) Weight change

3) Stereoscopic and scanning electron (SEM) microscopy

4) Optical metallography

5) KEVEX and Auger electron spectrochemical analysis.

### High Temperature Coupon Tests

Coupons of 304 stainless steel were immersed in liquid rubidium which partially filled sealed 25 $cm^3$ cylinders. The

atmosphere over the liquid Rb was argon with 0.3% total oxygen. This oxygen content is typical of the krypton separation product. Tests were run at 793, 843, and 893 K for times between 25 and 1,400 hours. After exposure, the extent of corrosion damage was metallographically measured. The time-temperature-penetration data were used to estimate the corrosion kinetics. Corrosion products were also chemically analyzed as described in the section on "C" ring tests.

## RESULTS

### "C" Ring Results

Significant general results of "C" ring tests at 400-672 K include:

1) No liquid metal embrittlement for any candidate material.

2) No corrosion damage for:

| | |
|---|---|
| 316 stainless steel | A286 |
| 347 stainless steel | Monel 400 |
| Nitronic 50 | Inconel 600 |

3) Pitting attack was observed at all temperatures for 4130 steel and 304 stainless steel.

The severity of pitting was metallographically analyzed as recommended in ASTM Standard G-47. Potentially injurious pitting may occur for 304 stainless steel at 672 K.

Metallographic and chemical analyses showed that pit initiation in 4130 steel was associated with sulfide inclusions. Sulfide inclusions are also known to be pit initiation sites in 4130 steel exposed to liquid lithium (3). In the case of liquid rubidium, initiation may result from the reaction:

$$MnS + 2Rb = Mn + Rb_2S$$

### Coupon Test Results

All specimens developed a thick external corrosion scale when exposed to rubidium at temperatures between 793 and 893 K. Examination of polished metallographic sections of the coupons showed the exterior corrosion product consisted of three layers. An example of this layering is shown in Figure 1. Results of KEVEX chemical analyses performed on the external corrosion

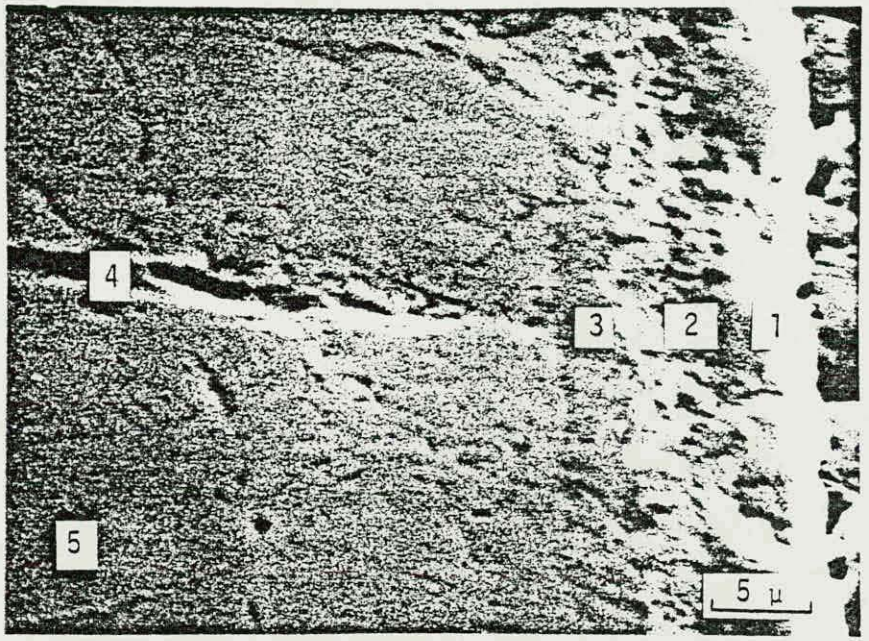


Figure 1. SEM Photograph of Polished Type 304 Stainless Steel Exposed to Rubidium at 843 K, Showing Three Layers of Outer Scale (1, 2, 3,) and Intergranular Attack (4). Spot Analysis of Base Metal was Made at Point (5).

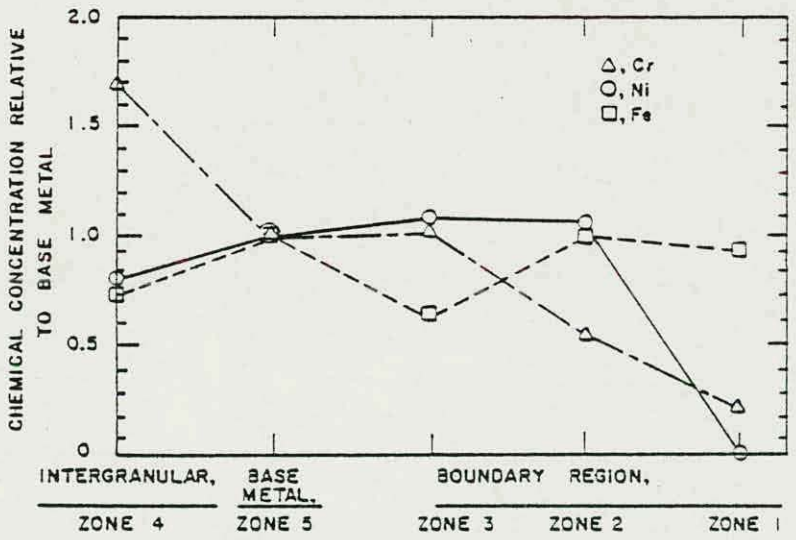


Figure 2. Chemical Analysis of Corrosion on Type 304 Stainless Steel Exposed to Rubidium at 843 K. Zone Numbers Correspond to Regions Shown on Figure 1.

product are summarized in Figure 2, which plots intensity ratios for iron, nickel, and chromium in each layer of the corrosion product relative to the base alloy. The outer layer, zone 1, consists mainly of iron and rubidium, with some chromium but no nickel. The central layer, zone 2, is rich in iron and nickel but is depleted with respect to chromium. The inner layer, zone 3, contains approximately the bulk levels of nickel and chromium but is depleted in iron. From these chemical results it appears that the processes active during general corrosive attack of 304 stainless steel involve (a) leaching of iron from the alloy, and (b) transport of iron away from the leading edge of attack.

A simple approach was used to estimate the external corrosion rate. The maximum corrosion penetration was metallographically measured on polished samples which incorporated the thickness of all three external corrosion layers. The rate of external corrosion was determined by two techniques: the infinite system "erf" solution and the thin film "exp" solution (4). Both analytical techniques gave similar results. The rate constant for external general corrosion in the temperature range 793 to 893 K was found to vary between $10^{-14}$ and $10^{-13}$ $cm^2/s$. The activation energy was 50 ± 3 kcal/mole. From this preliminary analysis it appears that the general corrosion rate is controlled by a solid state volume diffusion process.

Significant intergranular attack occurred on all specimens exposed to rubidium at 793, 843, and 893 K. An example of this intergranular attack is shown in Figure 3. Penetration increased

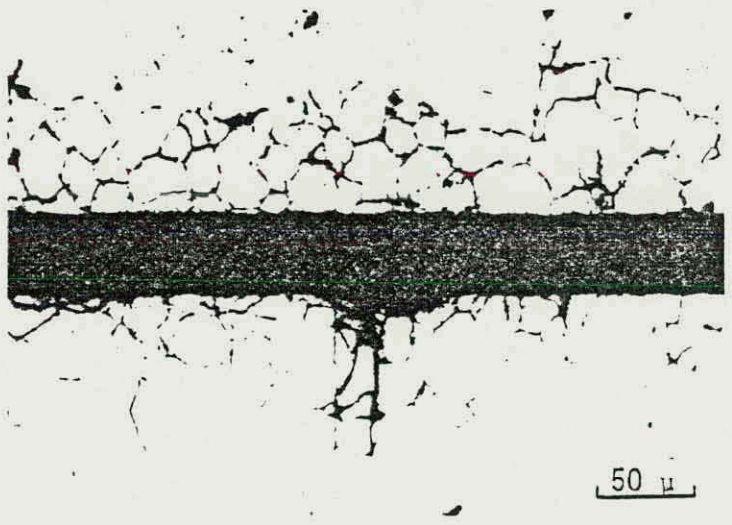


Figure 3. Metallographic Sections of Two Type 304 Stainless Steel Samples Exposed to 843 K Rubidium Showing Intergranular Corrosion.

with temperature. KEVEX analysis was also performed in regions of intergranular corrosion, such as spot 4 shown in Figure 1. The corroded grain boundary areas showed high relative concentrations of chromium. Typical intensity ratios in the grain boundary region compared to the unexposed bulk alloy were 1.7 for chromium, 0.75 for iron, and 0.80 for nickel. The observation of high chromium content along corroded grain-boundary paths is consistent with grain boundary sensitization of the 304 stainless steel.

The rate of intergranular penetration was significantly greater than the general corrosion rate. The rate constant for intergranular corrosion was determined using the Fisher solution for grain boundary diffusion (5). Preliminary calculations indicate that the rate constant varies between $10^{-9}$ and $10^{-8}$ $cm^2/s$ in the temperature range 793 to 893 K. This rapid grain boundary penetration appears to be related to sensitization of 304 stainless steel during corrosion testing at temperatures of 793 to 893 K.

Similar grain boundary corrosion effects have been reported for 304 stainless steel exposed to liquid lithium (6). Grain boundary corrosion in liquid lithium increases in the temperature range of sensitization. Also, the low-carbon and stabilized 300 series alloys exhibit superior resistance to grain boundary attack in lithium. For example, the rate constant for grain boundary penetration of 304L stainless steel in lithium at 893 K has been determined to be $8 \times 10^{-10}$ $cm^2/s$ (7). The slower rate of penetration in 304L stainless steel is attributed to a reduction in the level of sensitization compared to 304 stainless steel.

The mechanism of intergranular attack by rubidium in 304 stainless steel is complex. KEVEX chemical results indicate that accelerated corrosion along grain boundaries appears to result from leaching of iron by rubidium in the chromium-depleted zones at sensitized grain boundaries. However, the factors that lead to the initiation of intergranular corrosion have not been completely isolated. The two major test variables are temperature and rubidium purity. It has not been determined if temperature, and the resulting sensitization, cause the change in corrosion mode from pitting to general corrosion and intergranular penetration. The specific role of oxygen in rubidium corrosion is unknown, but it is expected that oxygen effects are significant as they are in liquid sodium (8).

## SUMMARY

Screening tests for eight materials in high purity rubidium showed no liquid metal embrittlement for statically stressed, smooth "C"-rings at temperatures between 400 and 672 K. Potentially

injurious localized corrosion in the form of pitting was observed for 304 stainless steel at 672 K. All other materials showed good performance in the temperature range proposed for krypton-85 gas cylinder storage.

Type 304 stainless steel showed significant general corrosion and intergranular attack in liquid rubidium of lower purity between 793 and 893 K. Type 304 stainless steel is not recommended for hardware which may encounter similar service conditions.

## REFERENCES


1. "Environmental Radiation Protection Standards for Nuclear Power Operations," Federal Register, Vol. 42, No. 9, Title 40, Part 190 (1977).

2. "ASTM Standard G-38," Annual ASTM Standards Part 10, ASTM (1977).

3. G. DeVries, "The Corrosion of Metals by Molten Lithium," in J. E. Draley and J. R. Weeks, Editors, Corrosion by Liquid Metals, pp. 251-269, Plenum Press (1970).

4. P. G. Shewman, Diffusion in Solids, pp. 6-15, McGraw-Hill (1963).

5. A. D. LeClaire, "The Analysis of Grain Boundary Diffusion Measurements," Brit. J. Appl. Phys. 14, 351-356 (1963).

6. R. Anderson and H. Stephen, "Progress Report on Materials Testing in Lithium," NEPA-1652, Oak Ridge National Laboratory (1950).

7. R. A. Patterson, R. J. Schlager, and D. L. Olson, "Lithium Grain Boundary Penetration of 304L Stainless Steel," J. of Nuclear Materials 57, 312-316 (1975).

8. W. F. Brehm, "Materials Compatibility in Liquid Sodium," HEDL-SA-1559, pp. 11-13, Hanford Engineering Development Laboratory (1978).